Available online at www.sciencedirect.com
ScienceDirect
Journal of Solid State Chemistry 179 (2006) 4003–4010
JOURNAL OF SOLID STATE CHEMISTRY
www.elsevier.com/locate/jssc

Three-dimensional molecular network, $[\{Cu(dps)_2(SO_4)\}\cdot 3H_2O\cdot DMF]_n$, and its different third-order NLO performance (dps = 4,4′-dipyridyl sulfide)

Yunyin Niu[a,*], Zhongjun Li, Yinglin Song[b], Mingsheng Tang[a], Benlai Wu[a], Xinquan Xin[c]

[a]*Department of Chemistry, Zhengzhou University, Henan Province 150001, Zhengzhou 450052, PR China*
[b]*Department of Applied Physics, Harbin Institute of Technology, Harbin 150001, PR China*
[c]*State Key Laboratory of Coordination Chemistry, Coordination Chemistry Institute, Nanjing University, Nanjing 210093, PR China*

Received 17 June 2006; received in revised form 31 August 2006; accepted 11 September 2006
Available online 17 September 2006

Abstract

A new three-dimensional non-interpenetrating coordination polymer, $[\{Cu(dps)_2(SO_4)\}\cdot 3H_2O\cdot DMF]_n$ (**1**) (dps = 4,4′-dipyridyl sulfide) was synthesized and structurally characterized. **1** crystallizes in triclinic system, space group $P\bar{1}$ with cell parameters of $a = 10.9412(1)$ Å, $b = 11.8999(1)$ Å, $c = 12.5057(1)$ Å, $V = 1400.7(3)$ Å^3, $Z = 2$, $D_c = 1.573\,g\,cm^{-3}$, $F(0\ 0\ 0) = 686$, $\mu = 1.059\,mm^{-1}$. $R_1 = 0.0436$, $wR_2 = 0.1148$. In the polymeric architecture, SO_4^{2-} serve as bridging coligands to connect highly puckered $[Cu_2(dps)_2]_n$ frameworks resulting in a 3D motif containing channels for guest molecule inclusion. Quantum chemistry calculation shows that the third-order NLO properties of polymer **1** are controlled by SO_4^{2-} groups and dps ligands, and metal ions have less influence on the third-order NLO properties.

Keywords: Coordination polymer; Copper(II) sulphate; 4,4′-dipyridyl sulfide; Nonlinear optical effect

1. Introduction

The crystal engineering of coordination polymers based on covalent interactions is an expanding field of research [1]. Crystallization of specifically building blocks combined with modulated fine factors has resulted in a number of new cavity materials [2]. An attractive concept in designing coordination crystals with large pores has been the formation of high dimensional networks. Among various types of these networks, the coordination polymers with 3D channels topology are of particular interest due to their desirable pore size and selective inclusion of guest molecules [2e, f]. However, the reported 3D coordination polymers are mostly ubiquitous interpenetrating networks [3],which have either very small pores or no pores at all. This decreases the potential uses as functional materials. Noninterpenetrating coordination polymers with well-defined large pores are therefore particularly desired. The discovery of noninterpenetrating molecular frames is still serendipitous since the structures were found to depend on several factors such as the supramolecular weak interactions, the nature or ratio of the ligands and the metals, and the presence of guest molecules [4]. Among various types of spacing ligands, 4,4′-dipyridyl sulfide (dps) possesses nonrigid backbone from a magic angle (C–S–C) bent around the sulfur atom and exhibits special adaptability for coordination requirements. Although dps has been exploited to produce a number of new coordination polymers [5], until now the 3D coordination complexes of it are much fewer [5h].

In this report, we chose $CuSO_4$ and dps as building blocks to describe the synthesis, structure and the nonlinear optical properties of the first 3D noninterpenetrating self-assembly of dps with $CuSO_4$.

*Corresponding author. Fax: +86 371 67767627.
E-mail address: niuyy@zzu.edu.cn (Y. Niu).

0022-4596/$ - see front matter © 2006 Elsevier Inc. All rights reserved.
doi:10.1016/j.jssc.2006.09.009

2. Experimental

2.1. Synthesis of $[\{Cu(dps)_2(SO_4)\}\cdot 3H_2O\cdot DMF]_n$ (1)

A solution of $CuSO_4\cdot 5H_2O$ (0.125 g, 0.5 mmol) in a methanol/water mixture (5:1, 5 mL) was allowed to diffuse slowly into a solution of 4,4′-dipyridylsulfide (0.188 g, 1 mmol) in DMF (5 mL). Deep blue crystals formed at the bottom of the solution after a month. Calcd. for $C_{23}H_{29}CuN_5O_8S_3$ (663.23)(%): Calcd. C 41.65, H 4.41, N 10.56; found C 41.31, H 4.52, N 10.57. IR(KBr pellet, cm^{-1}): 3549(br), 3471(sh), 3415(vs), 3235(w), 1619(s), 1475(w), 1402(s), 1213(w), 1130(m), 812(w), 725(w), 619(m). The X-ray powder diffraction pattern of the compound is in good agreement with the simulated one based on the single-crystal structure data, suggesting the purity of the synthesized sample (Fig. 1).

2.2. Characterization

4,4′-dipyridyl sulfide (dps) was obtained from Aldrich. Other chemicals were obtained from commercial sources and used as received. All solvents were predried over activated molecular sieves and refluxed over the appropriate drying agents under argon. The IR spectrum was recorded on a Shimazu IR435 spectrometer as KBr disk (4000–400 cm^{-1}). The X-ray powder diffraction patterns were recorded on a RIGAKU D/MAX-3B diffractometer by using Cu–Ka radiation ($k = 1.5418$ Å) with a graphite monochromator. The step size was 0.02° and the scan speed was 6°/min. The elemental analysis for C, H, and N were performed on a Perkin-Elmer 240C instrument.

2.3. X-ray structure determination

Crystallographic data for the title compound was collected at 291(2) K on a Bruker APEX-II area-detector diffractometer with Mo–Ka radiation ($\lambda = 0.71073$ Å). Absorption corrections were applied by using SADABS. The structure was solved with direct methods and refined with full-matrix least-squares techniques on F^2 using the SHELXTL program package [6]. All of the non-hydrogen atoms were refined anisotropically. The hydrogen atoms were assigned with common isotropic displacement factors

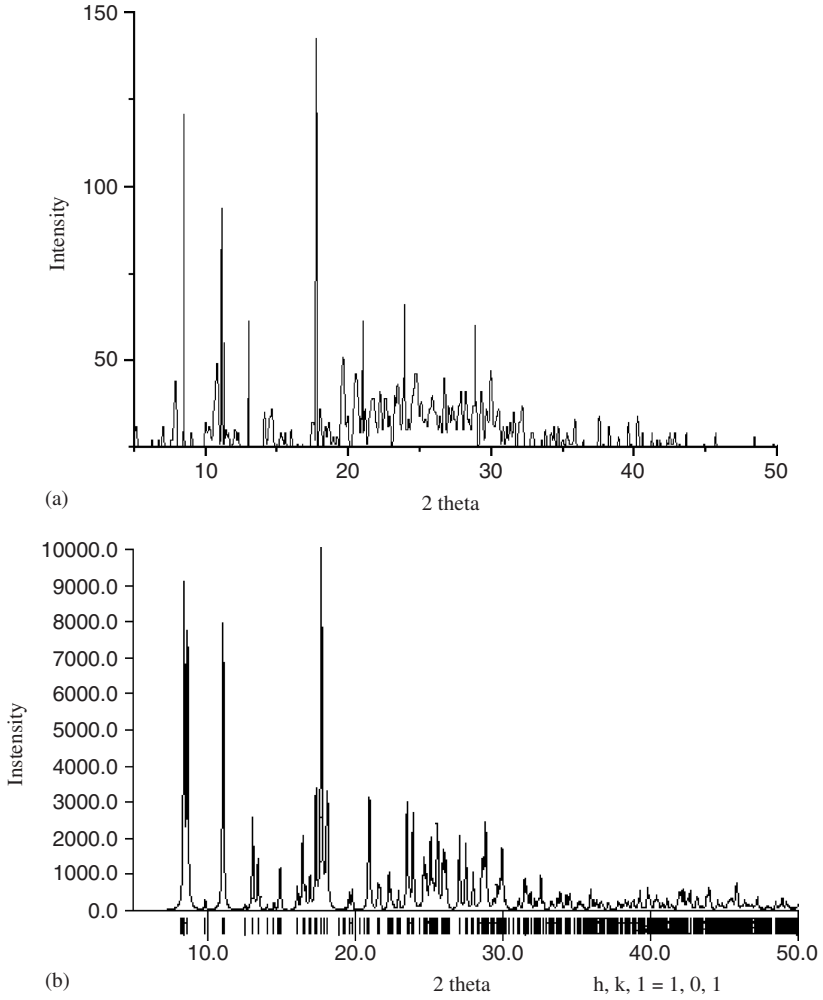

Fig. 1. (a) The experimental X-ray powder diffraction pattern of complex **1** and (b) the simulated pattern calculated from the single-crystal X-ray diffraction data of complex **1**.

and included in the final refinement by using geometrical restrains. Crystal data are summarized in detail in Table 1. Selected bond lengths and bond angles for **1** are put in Table 2.

Table 1
Crystal data and structure refinement summary for complex **1**

Empirical formula	$C_{23}H_{29}CuN_5O_8S_3$
Formula weight	663.23
Temperature (K)	291(2)
Wavelength (Å)	0.71073
Crystal system	Triclinic
Space group	P-1
a (Å)	10.941(1)
b (Å)	11.899(1)
c (Å)	12.506(1)
α (°)	64.312(2)
β (°)	74.123(2)
γ (°)	89.302(2)
Volume (Å^3)	1400.7(3)
Z	2
Calculated density (Mg m^{-3})	1.573
Absorption coefficient (mm^{-1})	1.059
F(0 0 0)	686
Crystal size (mm)	0.48 × 0.30 × 0.12
Theta range for data collection (°)	2.55–27.50
Limiting indices	$-13\leqslant h\leqslant 14$, $-15\leqslant k\leqslant 15$, $-16\leqslant l\leqslant 12$
Reflections collected/unique	8827/6206 [R(int) = 0.0204]
Completeness to $\theta = 27.50$	96.2%
Max. and min. transmission	0.8870 and 0.6320
Data/restraints/parameters	6206/9/382
Goodness-of-fit on F^2	1.059
Final R indices [$I>2\sigma(I)$]	$R_1 = 0.0436$[a], w$R_2 = 0.1148$[b]
R indices (all data)	$R_1 = 0.0562$, w$R_2 = 0.1248$
Largest diff. peak and hole (e Å^{-3})	1.004 and −0.656

$w = 1/[\sigma^2(F_o)^2 + .0297P^2 + 27.5680P]$ where $P = (F_o^2 + 2F_c^2)/3$.
[a] $R_1 = \big||F_o|-|F_c|\big|/|F_o|$.
[b] $wR_2 = \left[w\left(\left|F_o^2\right| - \left|F_c^2\right|\right)^2 / w\left|F_o^2\right|^2\right]^{1/2}$.

2.4. Nonlinear optical measurement

The optical measurements were performed with linearly polarized 8-ns pulses at 532 nm generated from a frequency-doubled Q-switched Nd:YAG laser, this wavelength is of paramount practical importance in the field of optical limiting as well as design and fabrication of resonance cavities of lasers. The spacial profiles of the pulses were nearly Gaussian after a spatial filter was employed. A DMF solution of compound **1** was placed in a 1-mm-thick quartz cell for optical limiting measurements. The crystal samples of it are stable toward oxygen, moisture and laser light. The laser pulse was focused into the cells containing the non-linear medium with a 250-mm focal length lens. The laser beam was divided into two beams. One was used to monitor the incident laser energy meter and the other was focused onto the sample cell. The input and the output energies of the beams were measured with an energy meter (Laser Precision Rjp-735) which were linked to a computer by an IEEE interface [7]. The experimental data were collected utilizing a single shot at a rate of 1 pulse per minute to avoid the influence of thermal effect.

3. Results and discussion

3.1. Description of the structure

X-ray crystallographic analysis revealed that the asymmetric unit of **1** contains two Cu atoms, two dps ligands, a SO_4^{2-} anion, a DMF and three H_2O molecules (Fig. 2). Each Cu(II) center is bonded to four different molecules of 4,4′-dipyridine sulfide and two sulfate anions in a six-coordinate manner. Four nitrogen atoms from four dps coordinate to the copper(II) center in the base plane, and

Table 2
Selected bond lengths (Å) and bond angles (°) for complex **1**

Cu(1)–N(1)	2.013(2)	Cu(1)–N(1)#1	2.013(2)
Cu(1)–N(4)#2	2.107(2)	Cu(1)–N(4)#3	2.107(2)
Cu(1)–O(1)	2.407(2)	Cu(1)–O(1)#1	2.407(2)
Cu(2)–N(2)	2.032(2)	Cu(2)–N(2)#4	2.032(2)
Cu(2)–N(3)#4	2.071(2)	Cu(2)–N(3)	2.071(2)
N(4)–Cu(1)#5	2.107(2)	N(1)–Cu(1)–N(1)#1	179.999(1)
N(1)–Cu(1)–N(4)#2	90.08(8)	N(1)#1–Cu(1)–N(4)#2	89.93(8)
N(1)–Cu(1)–N(4)#3	89.92(8)	N(1)#1–Cu(1)–N(4)#3	90.08(9)
N(4)#2–Cu(1)–N(4)#3	179.998(2)	N(1)–Cu(1)–O(1)	90.98(8)
N(1)#1–Cu(1)–O(1)	89.02(8)	N(4)#2–Cu(1)–O(1)	89.38(8)
N(4)#3–Cu(1)–O(1)	90.62(8)	N(1)–Cu(1)–O(1)#1	89.02(8)
N(1)#1–Cu(1)–O(1)#1	90.98(8)	N(4)#2–Cu(1)–O(1)#1	90.62(8)
N(4)#3–Cu(1)–O(1)#1	89.38(8)	O(1)–Cu(1)–O(1)#1	180.00(5)
N(2)–Cu(2)–N(2)#4	180.0	N(2)–Cu(2)–N(3)#4	87.65(8)
N(2)#4–Cu(2)–N(3)#4	92.35(8)	N(2)–Cu(2)–N(3)	92.35(8)
N(2)#4–Cu(2)–N(3)	87.64(8)	N(3)#4–Cu(2)–N(3)	180.0
C(5)–N(1)–Cu(1)	121.3(2)	C(1)–N(1)–Cu(1)	120.9(2)
C(19)–N(4)–Cu(1)#5	123.1(2)	C(18)–N(4)–Cu(1)#5	120.1(2)

Symmetry transformations used to generate equivalent atoms: #1: $-x+1$, $-y+1$, $-z+1$; #2: $-x$, $-y$, $-z+1$; #3: $x+1$, $y+1$, z; #4: $-x+1$, $-y$,$-z$; #5: $x-1$, $y-1$, z.

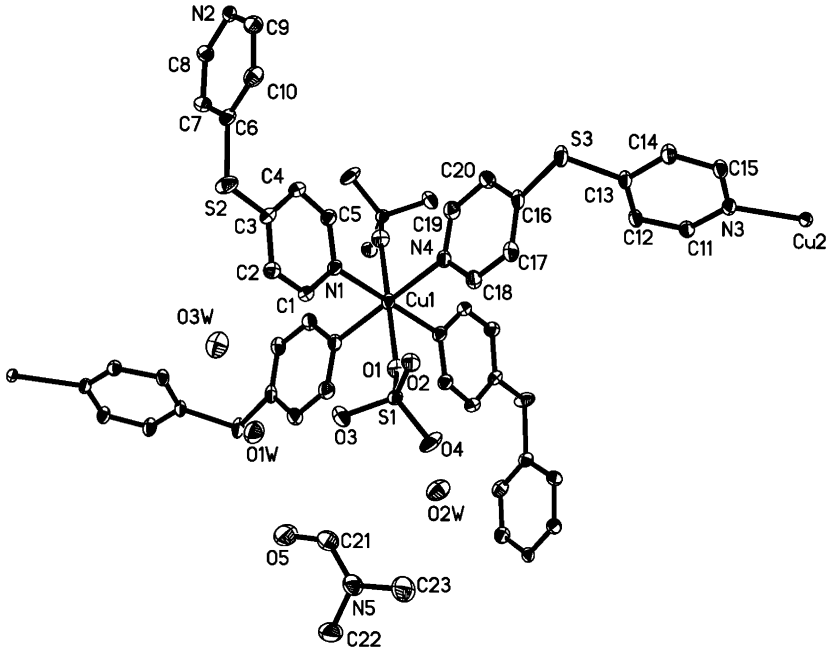

Fig. 2. An ORTEP drawing of the asymmetric unit and the copper (II) coordination environment in **1**.

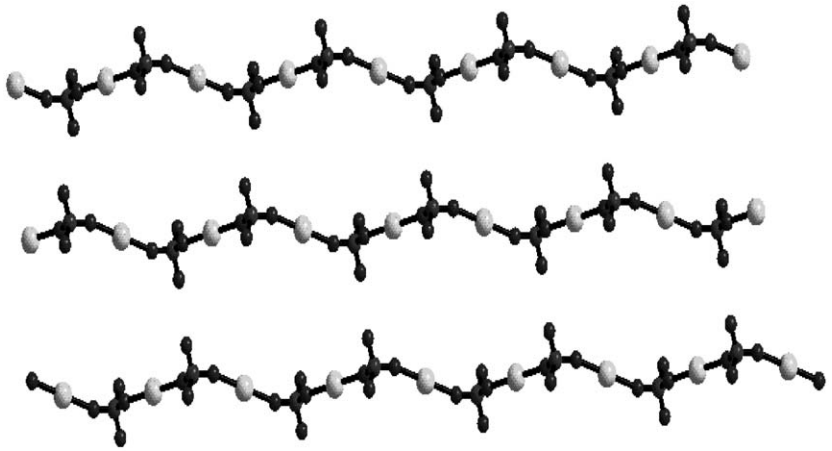

Fig. 3. A view of the 1D Cu–SO_4^{2-} polymeric chains along *c*-direction.

two oxygen atoms from two SO_4^{2-} are located in the axial positions of the distorted octahedral geometry of the copper(II). The Cu–N bond lengths are 2.013(2) and 2.107(2) Å, which are shorter than those (2.021(5) and 2.042(5) Å) in the 3D supramolecular array $\{[Cu(4,4'\text{-bipy})(H_2O)_3(SO_4)]\cdot 2H_2O\}_n$ (**2**) [4h] containing 1D linear coordination chains. The *cis* N–Cu–N and O–Cu–N bond angles vary from 89.02(8) to 90.98(8)°, and the *trans* $O(SO_4^{2-})$–Cu–$O(SO_4^{2-})$ bond angle is 180.00(5)° (Fig. 3). The axial Cu–μ–$O(SO_4^{2-})$ distance is 2.408(2) Å, which is also a little shorter than that found in **2** [Cu–*t*–$O(SO_4^{2-})$ = 2.663(5) Å].

There are two other closely related $CuSO_4$ self-assemblies with dps analogues: the 2D compound $\{[Cu(dpds)_2(SO_4)]\cdot 1.5H_2O\cdot CH_3OH\}_n$ (**3**) [8] (dpds = 4,4′-dipyridyl disulfide) and the 3D network compound $\{[Cu(dmps)_2SO_4]\cdot 0.5H_2O\cdot 0.5CH_2Cl_2\}_n$ (**4**) [9] (dmps = 4,4′-di(3-methyl) pyridyl sulfide). All the local bond parameters of **1** are similar to **3** and **4**. In **1** the Cu···Cu separation through the sulfate anion is 6.500 Å, which is a little shorter than that in 3 (7.118 Å). The Cu···Cu separations through the bridging ligand dps have two distances of 10.332 and 11.230 Å, while in **3** it is 10.547 Å. These variances can be attributed to the difference of ligand length between dps and dpds. Whereas in **4**, the similar skeletal length of dmps with dps only bring a similar Cu···Cu separation through the sulfate anion of 6.486 Å, and the Cu···Cu separation through the dmps is 10.892 Å, presumably due to the single C–S–C angle in dmps of 103.24(1)°. In striking contrast, in **1** the dps exhibits better flexibility and adopts two different geometry with two distinct C–S–C angles of 101.67(1) and 105.11(1)°, which bring two different Cu···Cu distances of

10.332 and 11.230 Å. Owing to the appropriate length and the bent geometry of the ligand, **1** adopts highly puckered interwoven geometry instead of interpenetration and no particular layer is displayed in the overall assembly (Fig. 4). In addition, the most fascinating feature of **1** is the occurrence of many three-dimensional channels formed by the coligand effects [5j] from metallacycles $[Cu_4(dps)_4]$ linked by the sulfate anions (Fig. 5), which provide cavities with sufficient size for the accommodation of H_2O and DMF molecules. In other case of absence of bridging anions, these metallacycles $[Cu_4(dps)_4]$ will became more regular and give square grids, such as coordination polymers $[Cu(dps)_2(PF_6)]_n$ and $[Cu(dps)_2(ClO_4)]_n$ [5]. In the molecular packing of **1**, there also exist supramolecular hydrogen interactions among dps, H_2O, and DMF molecules with C(dps)···O(DMF) distance of 3.177 Å, O(DMF)···O(H_2O) distance of 2.819 Å, and C(dps)–O(DMF)–O(H_2O) angles of 113.12°.

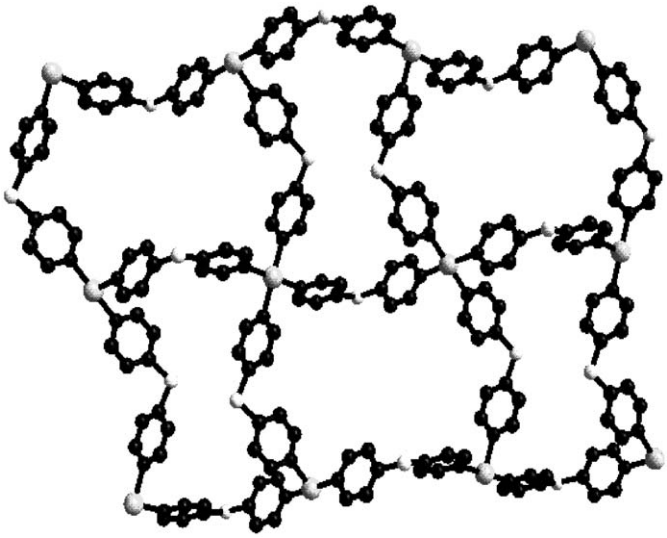

Fig. 4. A view of **1** along the *a*-axis that illustrates the highly puckered framework arrangement formed by copper with 4,4′-dipyridyl sulfide, the dimensions of the cavity is about 10.33×11.23 Å^2.

Fig. 5. A view of **1** along the *b*-axis that illustrates the 3D molecular channel formed by the metallacycles $[Cu_4(dps)_4]$ and the sulfate anions.

Among the available complexes of dps, the C–S–C angles range from 100.1° to 107.9° (Table 3). Based on the information in Table 3, metals preferring high coordination numbers often tend to form polymeric structures with high dimensionality, such as Co^{2+} complexes with 1–2D structures, and Cu^+ and Ag^+ complexes with 1–2D architectures. Whereas Zn^{2+} and Hg^{2+} complexes exhibit 0–1D structures for their tetrahedral preferences. So the metal ions' selection plays important role in the self-assembly reaction and has remarkable effect on the final dimensionality of polymeric complexes. The secondary factor is the number and size of terminal anions, the more they possess the terminal anions, the simpler the structure is; such as the related Ag complexes, $[Ag(NO_3)_3(dps)_2 \cdot 2H_2O]_n$ [5a], $[Ag_2(dps)_2(ClO_4)_2 \cdot (MeCN)]_n$ [5b], and $[Ag_2(dps)_2(MeCN)_3(ClO_4)_2 \cdot H_2O]_n$ [5b] are 1D structures, whereas $[Ag(dps)_2 \cdot BF_4]_n$ [5d], $[Ag(dps)_2(PF_6)]_n$ [5g], and $[Ag(dps)_2(CF_3SO_3)]_n$ [5g], are 2D. Another examples are $[Co(dps)_2(NCS)_2 \cdot 2H_2O]_n$ (1D) and $[Co(dps)_2Cl_2]_n$ (2D) [5j]: the NCS^- has bigger size and steric effect than Cl^-, and seems to be an obstacle to form 2D sheet. Compared with compound **2**, in **1** all the SO_4^{2-} serve as bridging ligands, and coligand effect facilitates the formation of the final 3D polymeric architecture.

All the results indicate that it is very important to choose building blocks for the construction of supramolecular structures. A preliminary conclusion can be drawn that the dimensionality and structure of self-assembled supramolecule depend mainly on three aspects: the coordination preferences of metal ion, the geometry, bulk, and rigidity of ligands, and the number and size of anions. So, if we want a self-assembly with complicated architecture, high coordination-number metal ion, multifunctional, flexible ligand, and skimpy anions is advisable in synthesis process.

3.2. Nonlinear optical effect and theoretical calculation

The third-order NLO studies of **1** were investigated in a 2.40×10^{-4} mol dm^{-3} DMF solution by *Z*-scan technique at 532 nm (Fig. 6). The results illustrate that the absorption is weak and the nonlinear optical properties are dominated by nonlinear refraction. The valley and peak occur at equal distances from the focus. This result is consistent with the notion that observed optical nonlinearity has an effective third-order dependence on the incident electromagnetic field [7a]. The valley/peak pattern of the normalized transmittance curve obtained under the closed aperture configuration shows characteristic self-focusing behavior of propagating light in the sample. However, when the *Z*-position is greater than 0 cm, the observed third-order NLO process is no longer pure third-order in nature, and

Table 3
The bent angle of the sulfur atom of dps in different compounds

Compound	Structure type	C–S–C (°)	Refs.
$[Ag_3(NO_3)_3(dps)_2 \cdot 2H_2O]_n$	1D double stranded	104.4–107.8	[5a]
$[Ag_2(dps)_2(ClO_4)_2\ (MeCN)]_n$	1D double stranded	107.2	[5b]
$[Ag_2(dps)_2(MeCN)_3(ClO_4)_2 \cdot H_2O]_n$	1D double stranded	107.4–107.9	[5b]
$[Zn(dps)(CH_3COO)_2]_n$	1D zigzag single stranded	103.4	[5b]
$[Zn(dps)_2(H_2O)_2(ClO_4)_2 \cdot H_2O]$	0D mononuclear complex	100.5–102.0	[5b]
$[Cu_2(dps)_2I_2]_n$	2D noninterpenetrating	102.5	[5b]
$(H_2dps)[CuCl_4]$	closed supramolecular	102.8	[5c]
$[Ag(dps)_2\cdots(BF_4)]_n$	2D noninterpenetrating	102.2–102.4	[5d]
$[Zn(dps)(CH_3COO)_2]_n$	1D linear	103.6	[5f]
$[Cu(dps)_2(ClO_4)]_n$	2D noninterpenetrating	103.6–103.8	[5g]
$[Cu(dps)_2(PF_6)]_n$	2D noninterpenetrating	100.6–105.0	[5g]
$[Ag(dps)_2(PF_6)]_n$	2D interpenetrating	102.8–105.8	[5g]
$[Ag(dps)_2(CF_3SO_3)]_n$	2D interpenetrating	102.3–105.4	[5g]
$[Cu_4(dps)_4(Mo_8O_{26}) \cdot 2H_2O]_n$	3D interpenetrating	99.3–100.5	[5h]
$[Co(dps)_2(NCS)_2 \cdot 2H_2O]_n$	1D double-stranded	100.1	[5j]
$[Co(dps)_2Cl_2]_n$	2D polycatenated	104.4	[5j]
$[Cu(dps)_2(SO_4) \cdot 3H_2O \cdot DMF]_n$	3D noninterpenetrating	101.67(1), 105.11(1)	This work

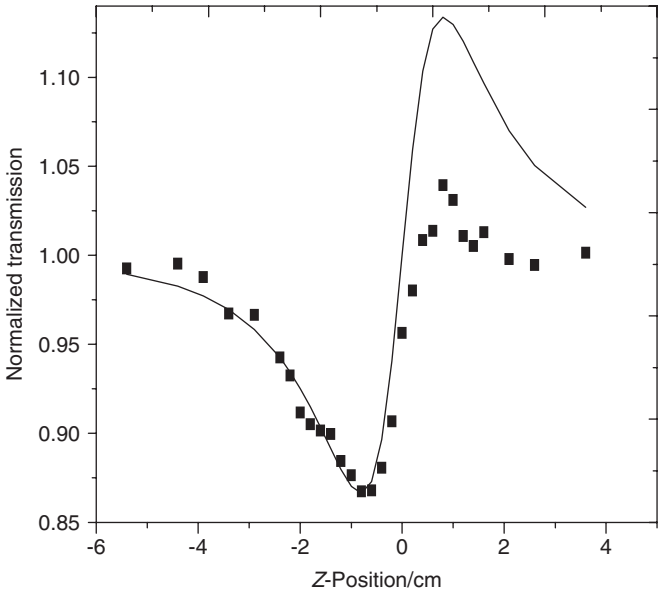

Fig. 6. The *Z*-scan data of **1** in DMF solution.

this deviate shows a different third-order NLO mechanism of **1** with other compounds.

Metal complexes of pyridine and bipyridine-type ligands represent an important class of nonlinear optical (NLO) materials [10], and combing bipyridyl ligands with metal ions is also an effective tool for tuning the nonlinear response [11]. There have been reports that dps ligand can be used as an organic emitting unit [5a, b]. In order to further investigate the contribution of metal ion and ligand to the third-order NLO properties. We use the Gaussian 03 suit of program to calculate frontier molecular orbitals by density functional theory (DFT) and analyze orbital occupied modulus of each part. The X-ray diffraction crystallographic data of complex **1** was utilized to establish the input atomic coordinates and calculated geometry [12]. Analysis of the energy characteristics was performed on the most stable structural unit using B3LYP functional. The basis set used for C, O, N and H atoms was 6–31G(d), while effective core potentials with a LanL2DZ basis set were employed for transition metal Cu atom. Results are showed in Fig. 7. Through calculation, we can know that the frontier molecular orbitals of polymer **1**, namely α-HOMO and β-HOMO, are primarily SO_4^{2-}-based orbitals, while α-LUMO, and β-LUMO, are primarily dps-based orbitals. Hence, according to quantum chemistry calculation, we can deduce that the third-order NLO properties of polymer **1** are controlled by two parts, namely SO_4^{2-} groups, and dps ligands. The metal atoms have less impact on the third-order NLO properties. We can also conclude that coordination polymer **1** has a different third-order NLO mechanism with that of clusters, which were also determined by metal atom centers, so called the heavy atom effects [13].

4. Conclusion

In summary, we designed and synthesized a new 3D polymeric complex, which exhibits third-order NLO properties. Coligand effects from the organic and inorganic bridging ligands can impart to the rational self-assemble of the high dimensional metal-based coordination polymers. In the self-assembly process although the mechanism of the anion contribution to architectures is manifestly unpredictable, understanding the key features may be a clue to the development of self-assembly composite materials that exhibit desirable properties. The non-linear refractive behaviors of the title polymer are mainly attributed to SO_4^{2-} groups and dps ligand, while the metal atom has less influence on the third-order NLO properties. It is clear that we need to accumulate more data for the third-order NLO study from more metal-organic polymers. Also further theoretical research will be needed to illuminate the

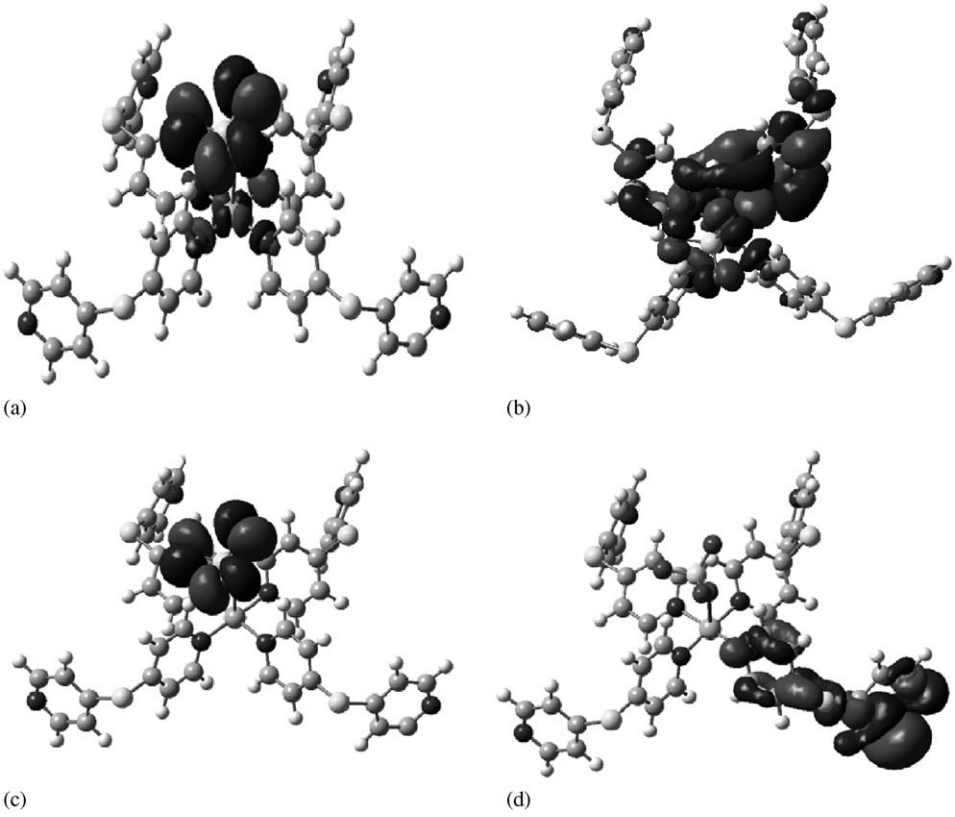

Fig. 7. The frontier molecular orbitals of polymer **1**: (a) α-HOMO, (b) α-LUMO, (c) β-HOMO, and (d) β-LUMO.

relationships between the structure, ligand, metal ion and third-order NLO properties.

Supporting information: CCDC-603121 contains the supplementary crystallographic data for (**1**). These data can be obtained free of charge via http://www.ccdc.cam.ac.uk/conts/retrieving.html, or from the Cambridge Crystallographic Data Centre, 12 Union Road, Cambridge CB2 1EZ, UK; fax: +44 1223 336 033; or E-mail: deposit@ccdc.cam.ac.uk.

Acknowledgments

This research was funded by the Science Foundation for Distinguished Young Scholars of Henan Province (Grant no. 0612002800) and the National Natural Science Foundation (Grant no. 20671083).

References

[1] (a) M. Fujita, Y.J. Kwon, S. Washizu, K. Ogura, J. Am. Chem. Soc. 116 (1994) 1151;
(b) S. Kitagawa, R. Kitaura, S.I. Noro, Angew. Chem. Int. Ed. 43 (2004) 2334.
[2] (a) J.A. Hanko, M.G. Kanatzidis, Angew. Chem. Intl. Ed. 37 (1998) 342;
(b) K. Biradha, K.C. Domasevitch, C. Hogg, B. Moulton, K.N. Power, M.J. Zaworotko, Cryst. Eng. 2 (1999) 37;
(c) I. Yamaguchi, K. Osakada, T. Yamamoto, J. Am. Chem. Soc. 118 (1996) 1811;
(d) Z. Shi, S. Feng, S. Gao, L. Zhang, G. Yang, J. Hua, Angew. Chem. Int. Ed. 39 (2000) 2325;
(e) L. Pan, B. Parker, X.Y. Huang, D.H. Olson, J.Y. Lee, J. Li, J. Am. Chem. Soc. 128 (2006) 4180;
(f) L. Pan, D.H. Olson, L.R. Ciemnolonski, R. Heddy, J. Li, Angew. Chem. Int. Ed. 45 (2006) 616.
[3] (a) S. Lopez, M. Kahraman, M. Harmata, S.W. Keller, Inorg. Chem. 36 (1997) 38;
(b) O.M. Yaghi, H. Li, J. Am. Chem. Soc. 117 (1995) 10401;
(c) L. Carlucci, G. Ciani, D.M. Proserpio, A. Sironi, Chem. Commun. (1996) 1393;
(d) P.C.M. Duncan, D.M.L. Goodgame, S. Menzer, D.J. Williams, Chem. Commun. (1996) 2127;
(e) M.A. Withersby, A.J. Blake, N.R. Champness, P. Hubberstey, W.S. Li, M. Schröder, Angew. Chem. Int. Ed. Engl. 36 (1997) 2327.
[4] (a) K.K. Rangan, P.N. Trikalitis, M.G. Kanatzidis, J. Am. Chem. Soc. 122 (2000) 10230;
(b) A.J. Blake, N.R. Champness, M. Crew, S. Parsons, New J. Chem. (1999) 13;
(c) O.M. Yaghi, H. Li, J. Am. Chem. Soc. 118 (1996) 295;
(d) M. Kondo, T. Yoshitomi, K. Seki, M. Matsuzaka, S. Kitagawa, Angew. Chem. Int. Ed. 36 (1997) 1725;
(e) T.L. Hennigar, D.C. MacQuarie, P. Losier, R.D. Rogers, M.J. Zaworotko, Angew. Chem. Int. Ed. 36 (1997) 972;
(f) J.I. Jay, C.W. Padgett, R.D.B. Walsh, T.W. Hanks, W.T. Pennington, Cryst. Growth Des. 1 (2001) 501;
(g) S.I. Noro, S. Kitagawa, M. Kondo, K.J. Seki, Angew. Chem. Int. Ed. 39 (2000) 2081;
(h) M.L. Tong, X.M. Chen, Cryst. Eng. Commun. 2 (2000) 1.

[5] (a) O.S. Jung, S.H. Park, C.H. Park, J.K. Park, Chem. Lett. 9 (1999) 923;
(b) S. Muthu, Z. Ni, J.J. Vittal, Inorg. Chim. Acta 358 (2005) 595;
(c) Y.H. Wen, J.K. Cheng, J. Zhang, Z.J. Li, Y.G. Yao, Acta Cryst. C 60 (2004) m618;
(d) O.S. Jung, S.H. Park, Y.A. Lee, U.K. Lee, Chem. Lett. 9 (2000) 1012;
(e) G.H. Zhao, X.S. Hu, P. Yu, H.K. Lin, Trans. Met. Chem. 29 (2004) 607;
(f) X.C. Su, Y.H. Guo, S.R. Zhu, H.K. Lin, J. Mol. Struct. 643 (2002) 147;
(g) Z. Ni, J.J. Vittal, Cryst. Growth Des. 1 (2001) 195;
(h) D. Hagrman, J. Zubieta, C.R. Acad. Sci., Serie IIc: Chim. 3 (2000) 231;
(i) G.H. Zhao, H.K. Lin, S.R. Zhu, H.W. Sun, Y.T. Chen, J. Coord. Chem. 46 (1998) 79;
(j) O.S. Jung, S.H. Park, D.C. Kim, K.M. Kim, Inorg. Chem. 37 (1998) 610.
[6] G.M. Sheldrick, SHELXL93, University of Göttingen, Germany, 1993.
[7] (a) M. Sheik-bahae, A.A. Said, T.H. Wei, D.J. Hangan, E.W. Van Stryland, IEEE J. Quant. Electron. 26 (1990) 760;
(b) M. Sheik-bahae, A.A. Said, E.W. Van Stryland, Opt. Lett. 14 (1989) 955.
[8] J.H. Luo, M.C. Hong, R.H. Wang, D.Q. Yuan, R. Cao, L. Han, Y.Q. Xu, Z.Z. Lin, Eur. J. Inorg. Chem. (2003) 3623.
[9] X.C. Su, S.R. Zhu, H.K. Lin, X.B. Leng, Y.T. Chen, J. Chem. Soc. Dalton Trans. (2001) 3163.
[10] H. Le Bozec, T. Renouard, Eur. J. Inorg. Chem. 2 (2000) 229.
[11] O. Maury, H. Le Bozec, Acc. Chem. Res. 9 (2005) 691.
[12] (a) H. Rensmo, S. Lunell, H. Siegbahn, J. Photochem. Photobiol. A. 114 (1998) 117;
(b) S.L. Zheng, X.M. Chen, Aust. J. Chem. 57 (2004) 703;
(c) C.X. Ren, B.H. Ye, F. He, L. Cheng, X.M. Chen, Cryst. Eng. Commun. 6 (2004) 200;
(d) D.Y. Wu, M. Hayashi, Y.J. Shiu, K.K. Liang, C.H. Chang, Y.L. Yeh, S.H. Lin, J. Phys. Chem. A 107 (2003) 9658.
[13] (a) Y.P. Sun, J.E. Riggs, Int. Rev. Phys. Chem. 18 (1999) 43;
(b) S. Shi, W. Ji, S.H. Tang, J.P. Lang, X.Q. Xin, J. Am. Chem. Soc. 116 (1994) 3615;
(c) S. Shi, W. Ji, J.P. Lang, X.Q. Xin, J. Phys. Chem. 98 (1994) 3570;
(d) C. Zhang, Y.L. Song, G.C. Jin, G.Y. Fang, Y.X. Wang, S.S.S. Raj, H.K. Fun, X.Q. Xin, J. Chem. Soc. Dalton Trans. (2000) 1317;
(e) C. Zhang, Y.L. Song, Y. Xu, H.K. Fun, G.Y. Fang, Y.X. Wang, X.Q. Xin, J. Chem. Soc. Dalton Trans. (2000) 2823.